Photon Counting Techniques for the Bandlimited Optical Channel

C. Lee, A. Gray
{clement, gray}@jpl.nasa.gov

Abstract—two methods of estimating received *photon counts* given a realistic noisy and bandlimited optical channel are presented. The function of estimating photon counts is critical in any optical communications receiver. The purpose of this work is to compare two methods—neither of which is generically optimal with realistic channels—for the purpose of assessing which is more appropriate for application in a hardware receiver given the current state-of-the art.

TABLE OF CONTENTS

1. Introduction

As part of NASA's Mars Laser Communications Demonstration (MLCD) project the Jet Propulsion Laboratory (JPL) is currently developing a pulse position modulation (PPM) laser communications receiver to support the future optical communications link to be demonstrated between Mars and Earth. The figure below is a typical model for a digital optical communication system [1].

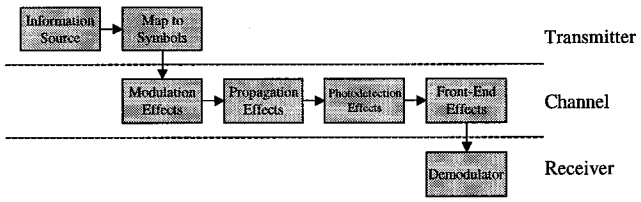

Figure 1: High-level system model

The PPM demodulator consists of photon counting within slot boundaries and finding the largest slot photon count within the symbol boundaries. This assumes that slot and symbol timing are both recovered and known [2]. Noise sources in optical communication systems include the following: quantum shot noise, optical excess noise, optical background noise, photodetector dark current noise, photodetector excess noise, and electronics (thermal) noise [1, 2].

In this paper we present and provide an analysis and comparison for the performance of two methods of estimating received photons given a noise channel, i.e. photon counting—one based on thresholding and the other on energy estimation using discrete-time samples—both of which result in a discrete-time estimate of the number of photons in some time epoch. From a communications systems perspective it is desirable for the detector to have infinite bandwidth—or at least not be the limiting bandwidth component in the system—and be noiseless. Unfortunately neither of these is necessarily true in practice. An analytical and a software model of a realistic detector is used in the performance comparison of both photon count estimations methods. The metric for comparing the two methods is itself an interesting topic and depends on the specific application of the optical system. Generic metrics are used in this work that are applicable to a large range of photon counting applications; the two metrics used are the total number of photons estimated versus actual number of photons received in some time epoch and the mean number of photons estimated versus the actual mean in that epoch. The time epoch is chosen to indicate performance over a long-time average. Better metrics may be used in certain applications. Both estimation methods have strengths and weaknesses that trade-off in the areas of performance and implementation complexity; in the conclusion a brief discussion of these trades is given using the performance comparison given herein.

2. Detector model

The output of the detector, $y(t)$, can be model by:

$$y(t) = \sum_{k=-\infty}^{\infty} \sum_{i=0}^{\lambda(k|\nu)-1} h(t - \tau_i - kT_{slot}), \quad (1)$$

where $\lambda(k)$, the number of photons that hit the detector, is a counting process, represented with a Poisson random variable [1,2]; τ is a uniform arrival time of the photon; T_{slot}

[1] 0-7803-8870-4/05/$20.00© 2005 IEEE
[2] IEEEAC paper #1403, 2004

is the slot duration; $h(t)$ is some arbitrary causal, band limited pulse response function, with the following constraints:

1.) $\int_{-\infty}^{\infty} h(t) > 0$

2.) pulsewidth of $h(t)$ < slot width, T_{slot}

3.) $h(t)$ is symmetric

For the purposes of this discussion, a truncated sinc function will be used to represent a causal pulse generated by a real detector.

$$h(t) = \begin{matrix} \sin(t)/t, & -\pi \le t \le 3\pi \\ 0, & else \end{matrix}$$

Ideally, $h(t)$ would be an impulse function. The bandwidth of $h(t)$ plays in important role in the trade offs of the two front end processing methods. Realistic detector output pulse widths range from several nanoseconds to as low as hundreds of picoseconds [3,4]. For the purposes of this discussion, we will assume a fixed slot width. Hence, the bandwidth of $h(t)$ will always be referred as a ratio of pulse width over slot width ratio. To account for PPM modulation, let $v \in \{0,1\}$. For background slots, $v = 0$ and for signal slots, $v = 1$. For the purposes of this discussion, we will assume that only the signal slots will have photons. Thus we will only be concerned about estimating photon counts in signal slots. It is easy to expand these results to background slots as well. Other noise sources will be added in a later discussion.

3. Threshold Photon Counting

Threshold photon counting is typically accomplished with an analog broadband thresholder followed by an analog integrator. A mathematical model of threshold photon counting can be represented in the following way.

$$\eta(t) = \begin{cases} 1, & y(t) \ge \gamma \cap y(t-\Delta t) < \gamma \\ 0, & else \end{cases}$$

$$\hat{\lambda}(k \mid v) = \int_{(k-1)T_{slot}}^{kT_{slot}} \eta(t)dt$$

where $\eta(t)$ detects a rising edge of $y(t)$ that triggers threshold γ, Δt is a parameter based on the bandwidth of the analog edge detector. The bandwidth of the analog edge detector is assumed to be greater than the bandwidth of $h(t)$.

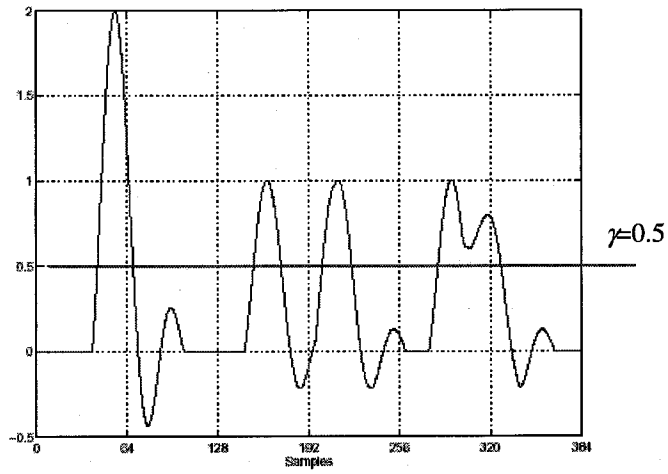

Figure 2: Threshold method will count only 4 out of 6 photons

Reference [5] describes photon counting of an APD detector using with an analog thresholder or discriminator.

4. Slot Energy Photon Counting

The front-end signal processing of an optical PPM receiver can use slot energy to determine the number photons in a given slot. The signal in the k^{th} slot is

$$y_k(t) = \sum_{i=1}^{\lambda(k|v)} h(t - \tau_i - kT_{slot})$$

Slot energy is estimated by summing the sampled detector output, resulting in $w(k)$. T_S is the sample period.

$$w(k) = \sum_{m=1}^{T_{slot}/T_S} y_k(mT_S) = \sum_{m=1}^{T_{slot}/T_S} \left[\sum_{i=1}^{\lambda(k|v)} h(mT_S - \tau_i - kT_{slot}) \right]$$

The slot photon count can then be recovered by normalizing with gain, G, and rounding to the nearest integer.

$$\hat{\lambda}(k \mid v) = round\left\{ \frac{w(k)}{G} \right\}, \quad (2)$$

Equation (2) is the slot energy estimate of the number of photons hitting the detector.

5. Estimating parameters

Determining the threshold to be used in the threshold photon counting processing can be solved analytically or empirically. The location of the threshold can be determined empirically by plotting the number of photon counts as a function of threshold assuming one photon in a slot. An ad-hoc threshold for single photon events in a slot is the mid point where the count is constant or flat over some range of thresholds. This empirical solution resulted in a $\gamma \approx 0.5$. See figure 3 below.

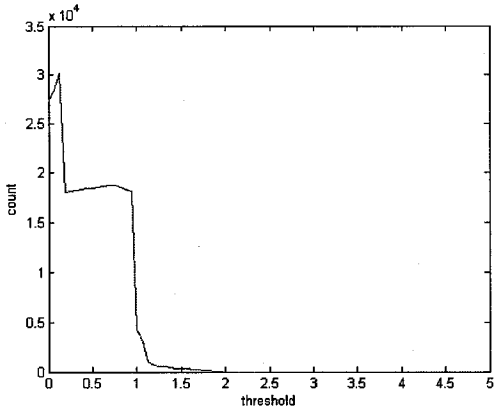

Figure 3: Photon count vs. threshold

Slot energy photon counting relies on gain, G, to map the energy of $h(t)$ to a photon count. This is a parameter that needs to be estimated prior to estimating photon counts. G can be estimated in several ways. The first is an expectation with respect to the random photon arrival time assuming exactly one photon per slot.

$$\hat{G} = E\{w(k)|\lambda = 1\} = E\left\{\sum_{m=1}^{T_{slot}/T_S} h(mT_S - \tau_k - kT_{slot})\right\} \quad (3)$$

The second method of estimating G is as follows. Let $\overline{\lambda}(k \mid v)$ be the mean of $\lambda(k \mid v)$. Define

$$\tilde{\lambda}(k) = \frac{w(k)}{G}$$

as the "soft value" photon count. We know that $\lambda(k)$ has a Poisson distribution. Let's assume that the "soft" count, $\tilde{\lambda}(k)$, is also Poisson. Thus the following can be assumed

$$E\{\tilde{\lambda}(k)\} = \mathrm{var}\{\tilde{\lambda}(k)\}$$
$$E\{\tilde{\lambda}(k)\} = \frac{E\{w(k)\}}{G}$$
$$\mathrm{var}\{\tilde{\lambda}(k)\} = \frac{\mathrm{var}\{w(k)\}}{G^2}$$

Combining the above three equations results in an estimate for the mean photon count and an estimate of the gain.

$$\hat{\bar{\lambda}} = E\{\tilde{\lambda}(k)\} = \frac{E\{w(k)\}^2}{\mathrm{var}\{w(k)\}}$$
$$\hat{G} = \frac{E\{w(k)\}}{\hat{\bar{\lambda}}} = \frac{\mathrm{var}\{w(k)\}}{E\{w(k)\}} \quad (4)$$

Estimating the mean and the variance of the slot energy, $w(k)$, can result in an estimate of the gain, G, and the mean slot photon count, $\hat{\bar{\lambda}}$. The sample mean and sample variance are Maximum Likelihood (ML) estimates of a Poisson random variable. The sample mean is an unbiased estimator. The sample variance estimator is also an unbiased estimator if normalized by N-1 samples. Since $w(k)$ is not truly Poisson, the above estimators are not optimal but are ML motivated estimators. The variance or performance on the estimator is a function of the number of samples used in the sample mean and variance.

Table 1. Comparison of two $\hat{G}$ estimates at $n_b = 0$, $n_s = 1$, pulse/slot width = 0.25

N sample estimate	$\mathrm{var}(\hat{G})$ (eqn. 3)	$\mathrm{var}(\hat{G})$ (eqn. 4)
100	0.0555	5.8761
500	0.0129	1.2940
1000	0.0117	0.8948

Equation 3 is a better estimator for G, but it will require calibrating the link to generate single photon events only. This may not be feasible. Equation 4 will allow us to estimate G in the real time or on the fly. The quality of the estimate will depend on the number of samples used. The variance equation 4 is much larger because it is making an estimate on a random number of incoming signal photons.

6. ISI effects on slot energy photon counting

The arrival time of each pulse is modeled as a uniform distribution over the time interval [0, T_{slot}] and the pulses at the output of the detector have some non-zero time extent (finite bandwidth) and thus it is possible for the photons within a single slot to overlap or the pulse in one slot to overlap with the pulse that is in another adjacent slot (even in the case of one photon per slot), the result of this latter is termed inter-symbol interference (ISI). This type of uncontrolled ISI—as opposed to controlled or designed ISI—may cause significant loss in a communications system; for simplicity here we are focused on the loss of estimating photon count per slot averaged over some time for the two methods outlined earlier. The most important effect of ISI on communications performance—namely impact on bit-error rate—must be determined in an end-to-end system (detector, receiver, and decoder); this work is deferred until a later date. Here we focus on the simple metrics of total estimated photon count per slot and estimated mean photons per slot averaged over a multiple of many slot periods. ISI increases as the pulse to slot width ratio increases due to bandlimted pulses.

ISI will also cause a bias in the slot phase, ϕ which will be a function of the pulse $h(t)$. This bias needs to be accounted for in the model in (1) in order to estimate photon count per slot precisely.

$$y_k(t) = \sum_{i=1}^{\lambda(k|v)} h(t - \tau_i - kT_{slot} - \phi)$$

For the specific pulse shape in figure 4, the bias is the pulsewidth/2.

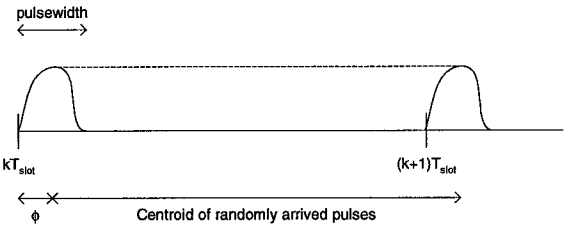

Figure 4: Slot sync loop will lock to centroid

This offset is used in the next section where the performance of estimating photon count is considered with and without the offset. Phase bias caused by ISI in threshold photon counting is negligible compared slot energy photon counting.

7. Photon Counting Performance

It is important to have some metric to quantify and compare the two front-end photon counters. Quantum Efficiency (QE) or Detection Efficiency (DE) is the metric used to determine the performance of photo detectors and is defined as [1,2]:

$$QE = \frac{Total\ number\ of\ photon\ triggered\ pulses}{Total\ number\ of\ incident\ photons}$$

We will use a similar metric to quantify the front end photon counters. Photon counting Efficiency (PCE) is defined as:

$$PCE = \frac{Total\ number\ of\ photon\ triggered\ pulses\ counted}{Total\ number\ of\ photon\ triggered\ pulses}$$

A photon counting front end processor that under counts photons will have a lower PCE. In theory, PCE and DE should not be larger than 1. The total efficiency of the detector, photon counter cascade is equal to the product of DE and PCE. The table below shows the PCE for a slot energy photon counter versus a threshold photon counter at various detector bandwidths quantified as a ratio: Pulse width/Slot width and various mean signal photons/slot (n_s). To simplify the problem, we will assume fixed PPM order of 4 and zero mean background photons/slot (i.e. $n_b = 0$). Simulations ran with 10000 symbols, with a sample rate of 128 times the slot rate.

Table 2. PCE of threshold vs slot energy

n_s	Pulse/slot width	PCE	
		Threshold photon counter	Energy photon counter with ISI correction
1	0.0625	0.9342	0.9982
1	0.125	0.8811	0.9986
1	0.25	0.7944	0.9956
1	0.5	-	0.9862
1	0.75	-	0.9684
2	0.0625	0.8939	0.9975
2	0.125	0.8053	0.9968
2	0.25	0.6725	0.9920
2	0.5	-	0.9774
2	0.75	-	0.9590
3	0.0625	0.8531	0.9970
3	0.125	0.7339	0.9962
3	0.25	0.5650	0.9905
3	0.5	-	0.9732
3	0.75	-	0.9496
4	0.0625	0.8065	0.9975
4	0.125	0.6728	0.9955
4	0.25	0.4799	0.9894
4	0.5	-	0.9698
4	0.75	-	0.9473

It can be assumed that the threshold photon counter will have pulse width to slot width ratios no greater than 0.25, as an analog broadband system. We can already see enough degradation in pulse/slot width ratio of 0.125.

Higher pulse/slot width ratio means the back-end receiver sub-systems (i.e. slot synchronization, etc.) bandwidths can be lower. Slot energy photon counting will allow us to low pass filter into the signal band to eliminate noise. This can sometimes result in an effective gain in signal-to-noise ratio (SNR). This will also allow lower sampling rates for digital processing.

The threshold photon counting under counts the higher mean slot photon arrival rates. As more photons arrive, there is a higher probability of overlapping pulses. Lower bandwidth pulses also have the same problem for the threshold photon counter. A multi-threshold system can help to alleviate this problem. Both single threshold and multi threshold photon counters can only detect edges that cross some threshold. If two pulses occur next to each other forming one longer pulse with one rising edge, the threshold photon counter will only count one pulse. Higher photon rates have a higher probability of that occurrence. So threshold photon counters tend to under count, thus lowering the PCE.

As PCE approaches 1, the two distributions should over lap. See figure 5 below. As PCE decreases, the photon counter distribution should move further left.

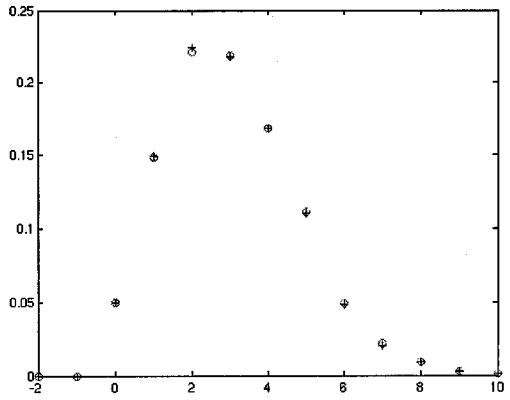

5(a) slot energy: PCE = 0.9962

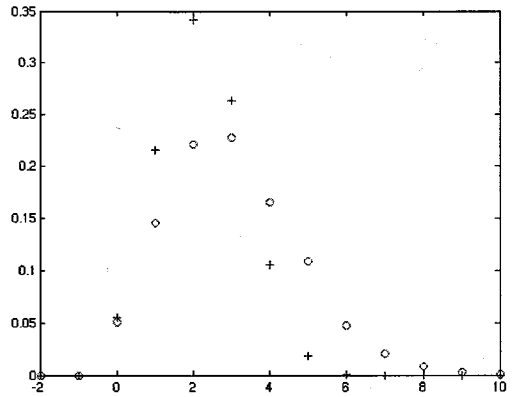

5 (b) threshold: PCE = 0.7339

Figure 5. signal slot count distribution: blue +: $\hat{\lambda}(k \mid \nu = 1)$, red o: $\lambda(k \mid \nu = 1)$ ($n_s = 3$, $n_b = 0$, pulse/slot ratio = 0.125)

8. Photodetection Noise Effects on Photon Counting Methods

A more realistic detector model factors in photodetector excess noise and thermal noise.

$$y(t) = \sum_{k=-\infty}^{\infty} \sum_{i=0}^{\lambda(k|\nu)-1} \alpha_i h(t - \tau_i - kT_{slot}) + n(t)$$

$n(t)$, represents thermal noise and is a Gaussian random variable with mean zero and variance σ^2 over the slot period; α represents random gain caused by photodetector excess noise, F, and has a gamma distribution with $E[\alpha] = ab = 1$ and $var[\alpha] = ab^2 = b$ and $F = 1 + var[\alpha]$.

The signal-to-thermal noise ratio is usually high for the photon-triggered pulses, due to the high gain from photon multiplication or avalanche effects of different photodetectors. Excess noise, F = 1.04, and thermal noise, slot σ^2 = 0.01 were modeled from a visible light photon counter (VLPC) detector and amplifier chain. Here are the results of noise using the above photon counting models.

Table 3. mean background slot photons (n_b) = 0

n_s	Pulse/slot width	PCE	
		Threshold photon counter	Energy photon counter with ISI correction
1	0.0625	0.9403	1.0079
1	0.125	0.8874	0.9957
1	0.25	0.7998	0.9901
1	0.5	-	0.9820
1	0.75	-	0.9545
4	0.0625	0.8102	0.9929
4	0.125	0.6720	0.9963
4	0.25	0.4897	0.9917
4	0.5	-	0.9678
4	0.75	-	0.9383

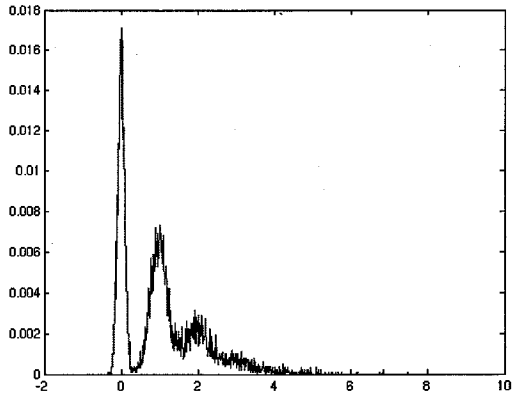

Figure 6. Histogram of soft photon counts in the signal slot ($n_s = 1$, $n_b = 0$, pulse/slot width = 0.125)

Figure 6 shows how thermal and excess noise spreads the distribution of the soft counts. The slot thermal noise variance can be approximated from the half width of the '0' peak. There is some degradation in PCE under the presence of noise. The next step is to vary the thermal noise variance to see the effect on PCE. This will be accomplished in a later discussion. Other optical channel effects can be added in a later discussion as well. Effects of dark current not modeled. Dark current rates are generally small, but will still skew the slot counts to be higher than they should be.

9. Conclusion

Photon counts derived from slot energy and threshold photon counting offer advantages and limitations that depend on the characteristics of the detector and channel. The results of this work indicate that threshold photon counting is best suited for a broadband detector, where current pulses approach an impulse function. In optical communications current pulses have high gain relative to the thermal noise floor, thus making thresholding a desirable approach to mitigate/eliminate thermal noise. The results further indicate that photon counting derived from slot energy estimates is best suited for a detector whose bandwidths are comparable to the digital system bandwidth. This method of photon counting also allows for counting of high slot photon count rates. Another photon counting method uses Fourier deconvolution to transform the current pulse $h(t)$ to an impulse [6]. The impulses can then be counted using a standard thresholder or discriminator. Some future work will involve comparing the performance of photon counts derived from slot energy estimates versus deconvolved thresholding photon counting.

ISI will reduce the estimation performance of both the energy and threshold methods. In general the more severe the ISI from bandlimiting—or alternatively the more "stretched" in time the pulse becomes—the greater the losses; thus for short slot periods Excess noise and thermal noise may become smaller contributors of estimation loss relative to the ISI. The work on determining the effects of ISI is deferred for future work.

References

[1] Stephen B. Alexander, *Optical Communication Receiver Design.* (Tutorial Texts in Optical Engineering Vol. TT22), SPIE-International Society for Optical Engine, 1997
[2] R.M. Gagliardi, S. Karp, Optical Communications, John Wiley & Sons, Inc., 1995.
[3] R.W. Engstrom, *Photomultiplier Handbook, Theory, Design, Application*, RCA, Princeton, NJ, 1980
[4] Hamamatsu Photonics K.K., Technical Data T-112-01, 1998
[5] X. Sun, F.M. Davidson, *Photon counting with silicon avalanche photodiodes*, Journal of Lightwave Technology, Vol. 10 No. 8, August 1992.
[6] D.V. Stoyanov, *Counting of overlapped photon detector single pulses by analog/digital sampling and deconvolution*, Optical Engineering, Vol. 36 No. 1, January 1997.

Bibliography

Clement Lee is in the Signal Processing Research Group in the Communications Architectures and Research Section. Mr. Lee has experience at JPL analyzing and designing a variety of signal processing systems ranging from reconfigurable radios and radar processing to optical communications receivers. Clement earned his MS in electrical engineering from the University of Southern California in 2003 and his BS in electrical engineering from University of California at Los Angeles in 1999.

Andrew Gray is a group supervisor of the Advanced Signal Processing Projects Group in the Communications Architectures and Research Section, and co-coordinator for the forward-looking Eureka Process that resides in the Mission and System Architecture Section at the Jet Propulsion Laboratory (JPL). Andrew earned his MBA and PhD in electrical engineering from the University of Southern California in 2004 and 2000 respectively, his MS in electrical engineering from the Johns Hopkins University in 1997, and his BS in electronics with minor in mathematics in 1994.

Photon Counting Techniques for the Bandlimited Optical Channel

C. Lee, A. Gray
{clement, gray}@jpl.nasa.gov

Abstract—two methods of estimating received *photon counts* given a realistic noisy and bandlimited optical channel are presented. The function of estimating photon counts is critical in any optical communications receiver. The purpose of this work is to compare two methods—neither of which is generically optimal with realistic channels—for the purpose of assessing which is more appropriate for application in a hardware receiver given the current state-of-the art.

TABLE OF CONTENTS

1. Introduction

As part of NASA's Mars Laser Communications Demonstration (MLCD) project the Jet Propulsion Laboratory (JPL) is currently developing a pulse position modulation (PPM) laser communications receiver to support the future optical communications link to be demonstrated between Mars and Earth. The figure below is a typical model for a digital optical communication system [1].

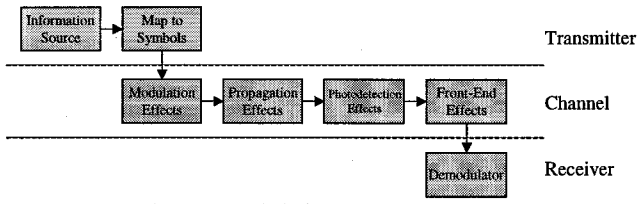

Figure 1: High-level system model

The PPM demodulator consists of photon counting within slot boundaries and finding the largest slot photon count within the symbol boundaries. This assumes that slot and symbol timing are both recovered and known [2]. Noise sources in optical communication systems include the following: quantum shot noise, optical excess noise, optical background noise, photodetector dark current noise, photodetector excess noise, and electronics (thermal) noise [1, 2].

In this paper we present and provide an analysis and comparison for the performance of two methods of estimating received photons given a noise channel, i.e. photon counting—one based on thresholding and the other on energy estimation using discrete-time samples—both of which result in a discrete-time estimate of the number of photons in some time epoch. From a communications systems perspective it is desirable for the detector to have infinite bandwidth—or at least not be the limiting bandwidth component in the system—and be noiseless. Unfortunately neither of these is necessarily true in practice. An analytical and a software model of a realistic detector is used in the performance comparison of both photon count estimations methods. The metric for comparing the two methods is itself an interesting topic and depends on the specific application of the optical system. Generic metrics are used in this work that are applicable to a large range of photon counting applications; the two metrics used are the total number of photons estimated versus actual number of photons received in some time epoch and the mean number of photons estimated versus the actual mean in that epoch. The time epoch is chosen to indicate performance over a long-time average. Better metrics may be used in certain applications. Both estimation methods have strengths and weaknesses that trade-off in the areas of performance and implementation complexity; in the conclusion a brief discussion of these trades is given using the performance comparison given herein.

2. Detector model

The output of the detector, $y(t)$, can be model by:

$$y(t) = \sum_{k=-\infty}^{\infty} \sum_{i=0}^{\lambda(k|\nu)-1} h(t - \tau_i - kT_{slot}), \quad (1)$$

where $\lambda(k)$, the number of photons that hit the detector, is a counting process, represented with a Poisson random variable [1,2]; τ is a uniform arrival time of the photon; T_{slot}

---

[1] 0-7803-8870-4/05/$20.00© 2005 IEEE

[2] IEEEAC paper #1403, 2004

is the slot duration; $h(t)$ is some arbitrary causal, band limited pulse response function, with the following constraints:

1.) $\int_{-\infty}^{\infty} h(t) > 0$

2.) pulsewidth of $h(t)$ < slot width, T_{slot}

3.) $h(t)$ is symmetric

For the purposes of this discussion, a truncated sinc function will be used to represent a causal pulse generated by a real detector.

$$h(t) = \begin{matrix} \sin(t)/t, & -\pi \le t \le 3\pi \\ 0, & else \end{matrix}$$

Ideally, $h(t)$ would be an impulse function. The bandwidth of $h(t)$ plays in important role in the trade offs of the two front end processing methods. Realistic detector output pulse widths range from several nanoseconds to as low as hundreds of picoseconds [3,4]. For the purposes of this discussion, we will assume a fixed slot width. Hence, the bandwidth of $h(t)$ will always be referred as a ratio of pulse width over slot width ratio. To account for PPM modulation, let $v \in \{0,1\}$. For background slots, $v = 0$ and for signal slots, $v = 1$. For the purposes of this discussion, we will assume that only the signal slots will have photons. Thus we will only be concerned about estimating photon counts in signal slots. It is easy to expand these results to background slots as well. Other noise sources will be added in a later discussion.

3. Threshold Photon Counting

Threshold photon counting is typically accomplished with an analog broadband thresholder followed by an analog integrator. A mathematical model of threshold photon counting can be represented in the following way.

$$\eta(t) = \begin{cases} 1, & y(t) \ge \gamma \cap y(t-\Delta t) < \gamma \\ 0, & else \end{cases}$$

$$\hat{\lambda}(k \mid v) = \int_{(k-1)T_{slot}}^{kT_{slot}} \eta(t)dt$$

where $\eta(t)$ detects a rising edge of $y(t)$ that triggers threshold γ, Δt is a parameter based on the bandwidth of the analog edge detector. The bandwidth of the analog edge detector is assumed to be greater than the bandwidth of $h(t)$.

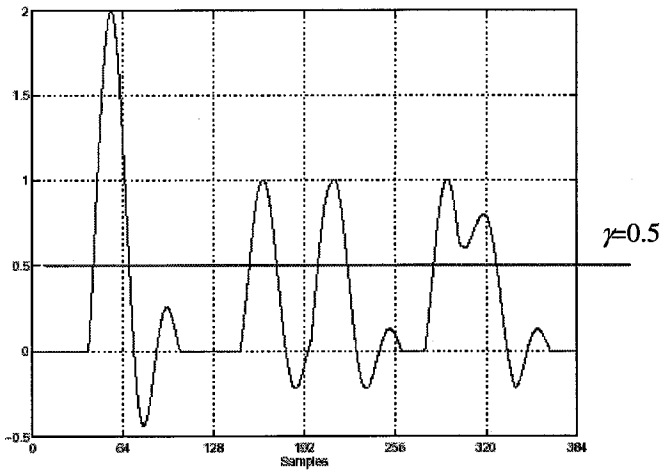

Figure 2: Threshold method will count only 4 out of 6 photons

Reference [5] describes photon counting of an APD detector using with an analog thresholder or discriminator.

4. Slot Energy Photon Counting

The front-end signal processing of an optical PPM receiver can use slot energy to determine the number photons in a given slot. The signal in the k^{th} slot is

$$y_k(t) = \sum_{i=1}^{\lambda(k|v)} h(t - \tau_i - kT_{slot})$$

Slot energy is estimated by summing the sampled detector output, resulting in $w(k)$. T_S is the sample period.

$$w(k) = \sum_{m=1}^{T_{slot}/T_S} y_k(mT_S) = \sum_{m=1}^{T_{slot}/T_S} \left[\sum_{i=1}^{\lambda(k|v)} h(mT_S - \tau_i - kT_{slot}) \right]$$

The slot photon count can then be recovered by normalizing with gain, G, and rounding to the nearest integer.

$$\hat{\lambda}(k \mid v) = round\left\{ \frac{w(k)}{G} \right\}, \quad (2)$$

Equation (2) is the slot energy estimate of the number of photons hitting the detector.

5. Estimating parameters

Determining the threshold to be used in the threshold photon counting processing can be solved analytically or empirically. The location of the threshold can be determined empirically by plotting the number of photon counts as a function of threshold assuming one photon in a slot. An ad-hoc threshold for single photon events in a slot is the mid point where the count is constant or flat over some range of thresholds. This empirical solution resulted in a $\gamma \approx 0.5$. See figure 3 below.

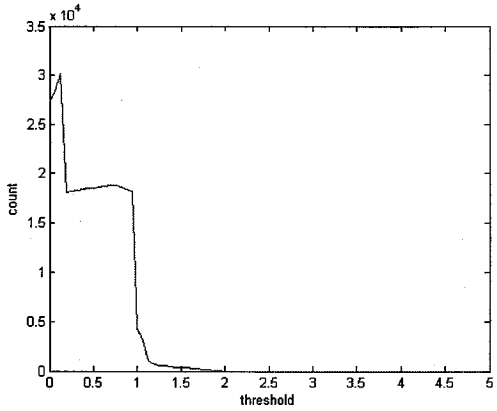

Figure 3: Photon count vs. threshold

Slot energy photon counting relies on gain, G, to map the energy of $h(t)$ to a photon count. This is a parameter that needs to be estimated prior to estimating photon counts. G can be estimated in several ways. The first is an expectation with respect to the random photon arrival time assuming exactly one photon per slot.

$$\hat{G} = E\{w(k)|\lambda = 1\} = E\left\{\sum_{m=1}^{T_{slot}/T_S} h(mT_S - \tau_k - kT_{slot})\right\} \quad (3)$$

The second method of estimating G is as follows. Let $\overline{\lambda}(k \mid v)$ be the mean of $\lambda(k \mid v)$. Define

$$\tilde{\lambda}(k) = \frac{w(k)}{G}$$

as the "soft value" photon count. We know that $\lambda(k)$ has a Poisson distribution. Let's assume that the "soft" count, $\tilde{\lambda}(k)$, is also Poisson. Thus the following can be assumed

$$E\{\tilde{\lambda}(k)\} = \text{var}\{\tilde{\lambda}(k)\}$$
$$E\{\tilde{\lambda}(k)\} = \frac{E\{w(k)\}}{G}$$
$$\text{var}\{\tilde{\lambda}(k)\} = \frac{\text{var}\{w(k)\}}{G^2}$$

Combining the above three equations results in an estimate for the mean photon count and an estimate of the gain.

$$\hat{\bar{\lambda}} = E\{\tilde{\lambda}(k)\} = \frac{E\{w(k)\}^2}{\text{var}\{w(k)\}}$$
$$\hat{G} = \frac{E\{w(k)\}}{\hat{\bar{\lambda}}} = \frac{\text{var}\{w(k)\}}{E\{w(k)\}} \quad (4)$$

Estimating the mean and the variance of the slot energy, $w(k)$, can result in an estimate of the gain, G, and the mean slot photon count, $\hat{\bar{\lambda}}$. The sample mean and sample variance are Maximum Likelihood (ML) estimates of a Poisson random variable. The sample mean is an unbiased estimator. The sample variance estimator is also an unbiased estimator if normalized by N-1 samples. Since $w(k)$ is not truly Poisson, the above estimators are not optimal but are ML motivated estimators. The variance or performance on the estimator is a function of the number of samples used in the sample mean and variance.

Table 1. Comparison of two $\hat{G}$ estimates at $n_b = 0$, $n_s = 1$, pulse/slot width = 0.25

N sample estimate	$\text{var}(\hat{G})$ (eqn. 3)	$\text{var}(\hat{G})$ (eqn. 4)
100	0.0555	5.8761
500	0.0129	1.2940
1000	0.0117	0.8948

Equation 3 is a better estimator for G, but it will require calibrating the link to generate single photon events only. This may not be feasible. Equation 4 will allow us to estimate G in the real time or on the fly. The quality of the estimate will depend on the number of samples used. The variance equation 4 is much larger because it is making an estimate on a random number of incoming signal photons.

6. ISI effects on slot energy photon counting

The arrival time of each pulse is modeled as a uniform distribution over the time interval [0, T_{slot}] and the pulses at the output of the detector have some non-zero time extent (finite bandwidth) and thus it is possible for the photons within a single slot to overlap or the pulse in one slot to overlap with the pulse that is in another adjacent slot (even in the case of one photon per slot), the result of this latter is termed inter-symbol interference (ISI). This type of uncontrolled ISI—as opposed to controlled or designed ISI—may cause significant loss in a communications system; for simplicity here we are focused on the loss of estimating photon count per slot averaged over some time for the two methods outlined earlier. The most important effect of ISI on communications performance—namely impact on bit-error rate—must be determined in an end-to-end system (detector, receiver, and decoder); this work is deferred until a later date. Here we focus on the simple metrics of total estimated photon count per slot and estimated mean photons per slot averaged over a multiple of many slot periods. ISI increases as the pulse to slot width ratio increases due to bandlimted pulses.

ISI will also cause a bias in the slot phase, ϕ which will be a function of the pulse $h(t)$. This bias needs to be accounted for in the model in (1) in order to estimate photon count per slot precisely.

$$y_k(t) = \sum_{i=1}^{\lambda(k|v)} h(t - \tau_i - kT_{slot} - \phi)$$

For the specific pulse shape in figure 4, the bias is the pulsewidth/2.

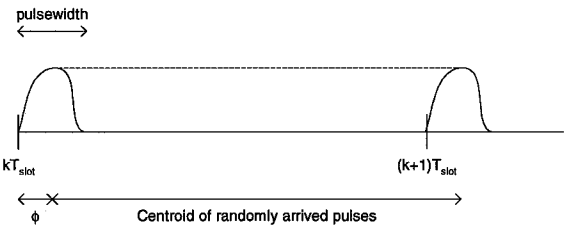

Figure 4: Slot sync loop will lock to centroid

This offset is used in the next section where the performance of estimating photon count is considered with and without the offset. Phase bias caused by ISI in threshold photon counting is negligible compared slot energy photon counting.

7. Photon Counting Performance

It is important to have some metric to quantify and compare the two front-end photon counters. Quantum Efficiency (QE) or Detection Efficiency (DE) is the metric used to determine the performance of photo detectors and is defined as [1,2]:

$$QE = \frac{Total\ number\ of\ photon\ triggered\ pulses}{Total\ number\ of\ incident\ photons}$$

We will use a similar metric to quantify the front end photon counters. Photon counting Efficiency (PCE) is defined as:

$$PCE = \frac{Total\ number\ of\ photon\ triggered\ pulses\ counted}{Total\ number\ of\ photon\ triggered\ pulses}$$

A photon counting front end processor that under counts photons will have a lower PCE. In theory, PCE and DE should not be larger than 1. The total efficiency of the detector, photon counter cascade is equal to the product of DE and PCE. The table below shows the PCE for a slot energy photon counter versus a threshold photon counter at various detector bandwidths quantified as a ratio: Pulse width/Slot width and various mean signal photons/slot (n_s). To simplify the problem, we will assume fixed PPM order of 4 and zero mean background photons/slot (i.e. n_b = 0). Simulations ran with 10000 symbols, with a sample rate of 128 times the slot rate.

Table 2. PCE of threshold vs slot energy

n_s	Pulse/slot width	PCE	
		Threshold photon counter	Energy photon counter with ISI correction
1	0.0625	0.9342	0.9982
1	0.125	0.8811	0.9986
1	0.25	0.7944	0.9956
1	0.5	-	0.9862
1	0.75	-	0.9684
2	0.0625	0.8939	0.9975
2	0.125	0.8053	0.9968
2	0.25	0.6725	0.9920
2	0.5	-	0.9774
2	0.75	-	0.9590
3	0.0625	0.8531	0.9970
3	0.125	0.7339	0.9962
3	0.25	0.5650	0.9905
3	0.5	-	0.9732
3	0.75	-	0.9496
4	0.0625	0.8065	0.9975
4	0.125	0.6728	0.9955
4	0.25	0.4799	0.9894
4	0.5	-	0.9698
4	0.75	-	0.9473

It can be assumed that the threshold photon counter will have pulse width to slot width ratios no greater than 0.25, as an analog broadband system. We can already see enough degradation in pulse/slot width ratio of 0.125.

Higher pulse/slot width ratio means the back-end receiver sub-systems (i.e. slot synchronization, etc.) bandwidths can be lower. Slot energy photon counting will allow us to low pass filter into the signal band to eliminate noise. This can sometimes result in an effective gain in signal-to-noise ratio (SNR). This will also allow lower sampling rates for digital processing.

The threshold photon counting under counts the higher mean slot photon arrival rates. As more photons arrive, there is a higher probability of overlapping pulses. Lower bandwidth pulses also have the same problem for the threshold photon counter. A multi-threshold system can help to alleviate this problem. Both single threshold and multi threshold photon counters can only detect edges that cross some threshold. If two pulses occur next to each other forming one longer pulse with one rising edge, the threshold photon counter will only count one pulse. Higher photon rates have a higher probability of that occurrence. So threshold photon counters tend to under count, thus lowering the PCE.

As PCE approaches 1, the two distributions should over lap. See figure 5 below. As PCE decreases, the photon counter distribution should move further left.

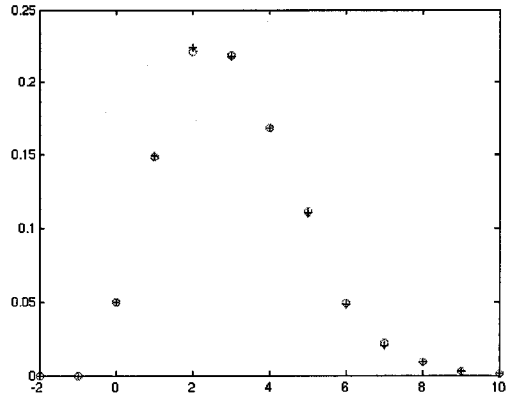

5(a) slot energy: PCE = 0.9962

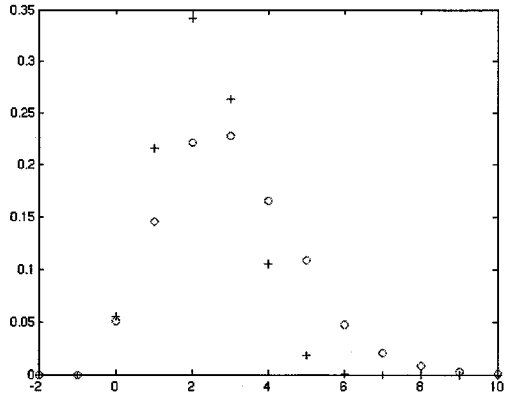

5 (b) threshold: PCE = 0.7339

Figure 5. signal slot count distribution: blue +: $\hat{\lambda}(k \mid \nu = 1)$, red o: $\lambda(k \mid \nu = 1)$ ($n_s = 3$, $n_b = 0$, pulse/slot ratio = 0.125)

8. Photodetection Noise Effects on Photon Counting Methods

A more realistic detector model factors in photodetector excess noise and thermal noise.

$$y(t) = \sum_{k=-\infty}^{\infty} \sum_{i=0}^{\lambda(k|\nu)-1} \alpha_i h(t - \tau_i - kT_{slot}) + n(t)$$

$n(t)$, represents thermal noise and is a Gaussian random variable with mean zero and variance σ^2 over the slot period; α represents random gain caused by photodetector excess noise, F, and has a gamma distribution with $E[\alpha] = ab = 1$ and $var[\alpha] = ab^2 = b$ and $F = 1 + var[\alpha]$.

The signal-to-thermal noise ratio is usually high for the photon-triggered pulses, due to the high gain from photon multiplication or avalanche effects of different photodetectors. Excess noise, F = 1.04, and thermal noise, slot σ^2 = 0.01 were modeled from a visible light photon counter (VLPC) detector and amplifier chain. Here are the results of noise using the above photon counting models.

Table 3. mean background slot photons (n_b) = 0

n_s	Pulse/slot width	PCE	
		Threshold photon counter	Energy photon counter with ISI correction
1	0.0625	0.9403	1.0079
1	0.125	0.8874	0.9957
1	0.25	0.7998	0.9901
1	0.5	-	0.9820
1	0.75	-	0.9545
4	0.0625	0.8102	0.9929
4	0.125	0.6720	0.9963
4	0.25	0.4897	0.9917
4	0.5	-	0.9678
4	0.75	-	0.9383

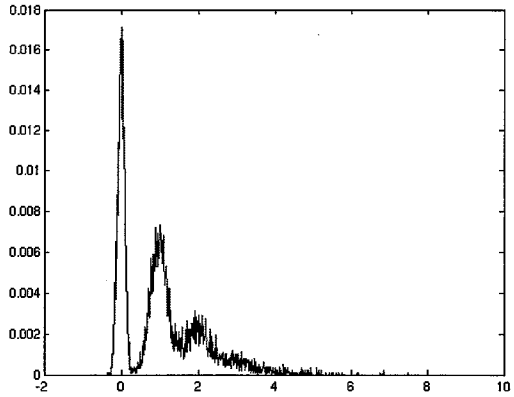

Figure 6. Histogram of soft photon counts in the signal slot ($n_s = 1$, $n_b = 0$, pulse/slot width = 0.125)

Figure 6 shows how thermal and excess noise spreads the distribution of the soft counts. The slot thermal noise variance can be approximated from the half width of the '0' peak. There is some degradation in PCE under the presence of noise. The next step is to vary the thermal noise variance to see the effect on PCE. This will be accomplished in a later discussion. Other optical channel effects can be added in a later discussion as well. Effects of dark current not modeled. Dark current rates are generally small, but will still skew the slot counts to be higher than they should be.

9. Conclusion

Photon counts derived from slot energy and threshold photon counting offer advantages and limitations that depend on the characteristics of the detector and channel. The results of this work indicate that threshold photon counting is best suited for a broadband detector, where current pulses approach an impulse function. In optical communications current pulses have high gain relative to the thermal noise floor, thus making thresholding a desirable approach to mitigate/eliminate thermal noise. The results further indicate that photon counting derived from slot energy estimates is best suited for a detector whose bandwidths are comparable to the digital system bandwidth. This method of photon counting also allows for counting of high slot photon count rates. Another photon counting method uses Fourier deconvolution to transform the current pulse $h(t)$ to an impulse [6]. The impulses can then be counted using a standard thresholder or discriminator. Some future work will involve comparing the performance of photon counts derived from slot energy estimates versus deconvolved thresholding photon counting.

ISI will reduce the estimation performance of both the energy and threshold methods. In general the more severe the ISI from bandlimiting—or alternatively the more "stretched" in time the pulse becomes—the greater the losses; thus for short slot periods Excess noise and thermal noise may become smaller contributors of estimation loss relative to the ISI. The work on determining the effects of ISI is deferred for future work.

References

[1] Stephen B. Alexander, *Optical Communication Receiver Design.* (Tutorial Texts in Optical Engineering Vol. TT22), SPIE-International Society for Optical Engine, 1997
[2] R.M. Gagliardi, S. Karp, Optical Communications, John Wiley & Sons, Inc., 1995.
[3] R.W. Engstrom, *Photomultiplier Handbook, Theory, Design, Application*, RCA, Princeton, NJ, 1980
[4] Hamamatsu Photonics K.K., Technical Data T-112-01, 1998
[5] X. Sun, F.M. Davidson, *Photon counting with silicon avalanche photodiodes*, Journal of Lightwave Technology, Vol. 10 No. 8, August 1992.
[6] D.V. Stoyanov, *Counting of overlapped photon detector single pulses by analog/digital sampling and deconvolution*, Optical Engineering, Vol. 36 No. 1, January 1997.

Bibliography

Clement Lee is in the Signal Processing Research Group in the Communications Architectures and Research Section. Mr. Lee has experience at JPL analyzing and designing a variety of signal processing systems ranging from reconfigurable radios and radar processing to optical communications receivers. Clement earned his MS in electrical engineering from the University of Southern California in 2003 and his BS in electrical engineering from University of California at Los Angeles in 1999.

Andrew Gray is a group supervisor of the Advanced Signal Processing Projects Group in the Communications Architectures and Research Section, and co-coordinator for the forward-looking Eureka Process that resides in the Mission and System Architecture Section at the Jet Propulsion Laboratory (JPL). Andrew earned his MBA and PhD in electrical engineering from the University of Southern California in 2004 and 2000 respectively, his MS in electrical engineering from the Johns Hopkins University in 1997, and his BS in electronics with minor in mathematics in 1994.